ACS SyntheticBiology

Research Article

pubs.acs.org/synthbio

Functional Exchangeability of Oxidase and Dehydrogenase Reactions in the Biosynthesis of Hydroxyphenylglycine, a Nonribosomal Peptide Building Block

Veronica Diez,[†,▽] Mark Loznik,[†,◆] Sandra Taylor,[∥] Michael Winn,[⊥] Nicholas J. W. Rattray,[⊥] Helen Podmore,[#] Jason Micklefield,[⊥] Royston Goodacre,[⊥] Marnix H. Medema,[†,¶] Ulrike Müller,[○] Roel Bovenberg,[○] Dick B. Janssen,[‡] and Eriko Takano*[,†,□]

[†]Department of Microbial Physiology, [‡]Department of Biochemistry, Synthetic Biology and Cell Engineering, Groningen Biomolecular Sciences and Biotechnology Institute, University of Groningen, 9747 AG Groningen, The Netherlands

Manchester Synthetic Biology Research Centre (SYNBIOCHEM), Manchester Institute of Biotechnology, [∥]Faculty of Life Sciences, [⊥]School of Chemistry, University of Manchester, 131 Princess Street, Manchester, M1 7DN, United Kingdom

[#]ThermoFisher Scientific, 1 Boundary Way, Hemel Hempstead, Herts, HP2 7GE, United Kingdom

[○]DSM Biotechnology Center, R&D, P.O. Box 1, 2600 AM Delft, The Netherlands

Supporting Information

ABSTRACT: A key problem in the engineering of pathways for the production of pharmaceutical compounds is the limited diversity of biosynthetic enzymes, which restricts the attainability of suitable traits such as less harmful byproducts, enhanced expression features, or different cofactor requirements. A promising synthetic biology approach is to redesign the biosynthetic pathway by replacing the native enzymes by heterologous proteins from unrelated pathways. In this study, we applied this method to effectively re-engineer the biosynthesis of hydroxyphenylglycine (HPG), a building block for the calcium-dependent antibiotic of *Streptomyces coelicolor*, a nonribosomal peptide. A key step in HPG biosynthesis is the conversion of 4-hydroxymandelate to 4-hydroxyphenylglyoxylate, catalyzed by hydroxymandelate oxidase (HmO), with concomitant generation of H_2O_2. The same reaction can also be catalyzed by O_2-independent mandelate dehydrogenase (MdlB), which is a catabolic enzyme involved in bacterial mandelate utilization. In this work, we engineered alternative HPG biosynthetic pathways by replacing the native HmO in *S. coelicolor* by both heterologous oxidases and MdlB dehydrogenases from various sources and confirmed the restoration of calcium-dependent antibiotic biosynthesis by biological and UHPLC-MS analysis. The alternative enzymes were isolated and kinetically characterized, confirming their divergent substrate specificities and catalytic mechanisms. These results demonstrate that heterologous enzymes with different physiological contexts can be used in a *Streptomyces* host to provide an expanded library of enzymatic reactions for a synthetic biology approach. This study thus broadens the options for the engineering of antibiotic production by using enzymes with different catalytic and structural features.

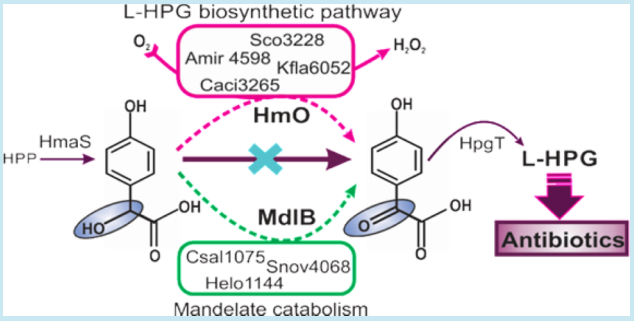

KEYWORDS: *synthetic biology, L-HPG biosynthesis, calcium-dependent antibiotics, nonribosomal peptide, HmO, MdlB, UHPLC-MS*

Among the major bottlenecks for the industrial production of antibacterial therapeutic compounds are the undesired catabolic and noncatabolic traits of the enzymes involved in the native biosynthetic pathways.[1] A key synthetic biology strategy to circumvent these difficulties is to redesign these biosynthetic pathways using enzymes that achieve the same function using different mechanisms and cofactors derived from unrelated physiological contexts, an approach that could give access, at the same time, to a multitude of novel or modified antibiotics with improved physicochemical and biological properties.[1,2]

Nonribosomal peptides (NRPs) are among the most widespread and complex secondary metabolites with key antibacterial activities. NRPs also have immunosuppressive, antitumor, antiviral, and antifungal activities.[3] The diversity of chemical structures and biological activities exhibited by NRPs is, in part, due to the incorporation of a wide range of nonproteinogenic amino acids, fatty acids, polyketide moieties, and glycosyl residues.[3]

The calcium-dependent antibiotic (CDA) from *Streptomyces coelicolor*[4,5] (Figure 1A) belongs to the group of acidic lipopeptide antibiotics including daptomycin, which, in 2003,

Received: January 29, 2014
Published: February 25, 2015

DOI: 10.1021/sb500368w
ACS Synth. Biol. 2015, 4, 796−807

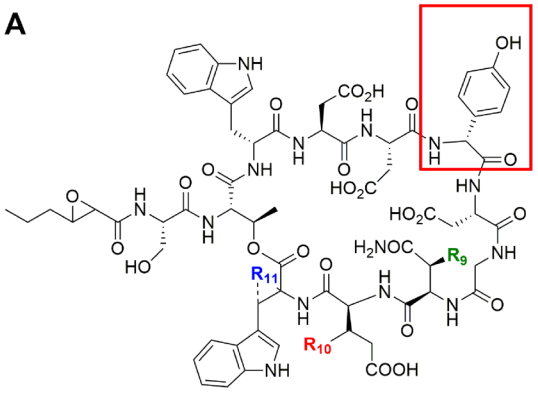

CDAx	R_9	R_{10}	R_{11}	Mol. wt.
CDA-1b	OPO_3H_2	H	H,H	1562
CDA-2a	OPO_3H_3	CH_3	π-bond	1574
CDA-2b	OPO_3H_4	CH_3	H,H	1576
CDA-3a	OH	H	π-bond	1480
CDA-3b	OH	H	H,H	1482
CDA-4a	OH	CH_3	π-bond	1494
CDA-4b	OH	CH_3	H,H	1496

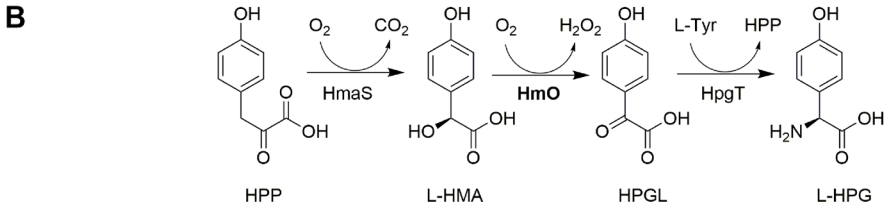

Figure 1. HPG is one of the components of CDA antibiotics. (A) Structure of the calcium-dependent antibiotic (CDA) from *S. coelicolor*.[4,5] D-4-Hydroxyphenylglycine (HPG) is highlighted with a red box. R indicates variability of amino acid residues at positions 9, 10, and 11. R_9 = OPO_3H_2 or OH; R_{10} = H or CH_3; R_{11} = H,H or π-bond.[4,5] (B) The L-HPG biosynthetic pathway. L-4-Hydroxymandelate synthase (HmaS) catalyzes the oxidative decarboxylation of 4-hydroxyphenylpyruvate (HPP) to L-4-hydroxymandelate (L-HMA), which, in turn, is oxidized to 4-hydroxyphenylglyoxylate (HPGL) by 4-hydroxymandelate oxidase (HmO). In this reaction, O_2 is reduced to H_2O_2. In the last step, HPGL is converted to L-HPG by a transamination reaction catalyzed by 4-hydroxyphenylglycine aminotransferase (HpgT). L-Tyrosine is used as an amino donor, thus regenerating HPP.

became the first example of a natural antimicrobial NRP to reach the clinic in over 30 years.[6] CDA contains a number of nonproteinogenic amino acids such as D-hydroxyphenylglycine (D-HPG), L-3-methylglutamic acid, a C-terminal Z-dehydrotryptophan residue, and modified asparagine residues,[4,7−10] all of which have been the target of numerous studies. The biosynthesis of the nonproteinogenic amino acid HPG is of particular interest, as this moiety also occurs in other bioactive compounds, such as vancomycin.[11] Branching from tyrosine catabolism, a novel and dedicated biosynthetic pathway for L-HPG has been reported in several actinomycetes[4,12−14] and more recently in nonactinomycete bacteria (Figure 1B).[15] The biosynthesis of L-HPG starts from 4-hydroxyphenylpyruvate, which is derived from tyrosine by a deaminating aminotransferase reaction. Conversion of hydroxyphenylpyruvate to L-HPG comprises the action of three enzymes: HmaS, catalyzing decarboxylation and oxidation to L-4-hydroxymandelate (L-HMA); hydroxymandelate oxidase HmO, catalyzing oxidation to 4-hydroxyphenylglyoxylate; and L-4-hydroxyphenylglycine aminotransferase (HpgT), involved in the transamination reaction yielding L-HPG. The presence of its stereoisomer, D-HPG, in the final lipopeptide antibiotic results from epimerization during peptide assembly by NRP synthetase.[4,12]

The second enzyme in the HPG biosynthetic pathway (HmO, Sco3228, UniProt Q9Z4X8) is a flavin mononucleotide (FMN)-dependent oxidase[12,16] that produces hydrogen peroxide, a potentially harmful byproduct if accumulated in high concentrations.[16] HmO oxidase shares amino acid sequence similarity to a FMN-containing mandelate dehydrogenase (MdlB, UniProt P20932) (50% amino acid (AA) similarity and 35% AA identity). MdlB is an O_2-independent enzyme from the mandelate pathway found in many strains of pseudomonads, and there is evidence that it also catalyzes the conversion of L-HMA to 4-hydroxyphenylglyoxylate.[17−19] While MdlB is a membrane-bound enzyme that reacts with a component of the electron transport chain (most probably ubiquinone), sequence comparison showed that the homologous O_2-dependent HmO is missing the membrane anchoring sequence (Supporting Information Figure S1, red box).[20,21] Although HmO and MdlB are evolutionarily related and both catalyze the conversion of L-4-hydroxymandelate to 4-hydroxyphenylglyoxylate, they have different electron-acceptor requirements and cellular localization. This raises the possibility of functional exchangeability in the process of re-engineering biosynthetic pathways. The exchange of enzyme building blocks with different catalytic and structural features can increase the productivity and diversity of target secondary metabolites.[1,2,22,23]

The aim of the present article is to show the interchangeability between oxidase and dehydrogenase enzymes during the biosynthesis of HPG-containing antibiotics. Homologues or orthologs that are distantly related to the *S. coelicolor* HmO protein or to MdlB were tested for their ability to complement the *hmO*-deficient *S. coelicolor* mutant. The results show that both types of enzymes are similarly capable of restoring CDA biosynthesis. Purification and detailed kinetic characterization of the different enzymes showed differences not only in relative stability but also in the substrate specificity of these orthologs. This article demonstrates that CDA biosynthesis can be catalyzed by a combination of biosynthetic and catabolic enzymes from unrelated metabolic pathways, giving rise to the possibility of expanding the library of enzymes that can be used

DOI: 10.1021/sb500368w
ACS Synth. Biol. 2015, 4, 796−807

in a synthetic biology approach for the future design of antimicrobial biosynthetic pathways.

RESULTS AND DISCUSSION

Deletion of the Hydroxymandelic Acid Oxidase-Encoding Gene, hmO. The FMN-dependent enzymes L-hydroxymandelate oxidase (HmO) and L-mandelate dehydrogenase (MdlB) both catalyze the conversion of 4-hydroxymandelic acid to 4-hydroxyphenylglyoxylate, but they originate from different metabolic pathways. Whereas HmO is involved in the production of NRPs, MdlB is part of the mandelate-utilization pathway.[12,16,24] In view of their similarity, the oxidation of the L-hydroxy acid to keto acid with the concomitant reduction of FMN is likely to proceed through the same mechanism. Seven active site residues, Tyr^{26}, Tyr^{131}, Asp^{158}, Arg^{165}, Lys^{249}, His^{273}, and Arg^{276}, which are highly conserved among the α-hydroxy acid oxidizing enzymes, are believed to be important for this reductive half-reaction (Supporting Information Figure S1, pink triangles).[25] However, the second half-reaction in which FMN is reoxidized is different for the two enzymes. HmO transfers two electrons and two protons from the reduced cofactor to molecular oxygen, generating hydrogen peroxide.[16] On the other hand, the bacterial membrane-bound MdlB transfers electrons to a component of the electron transport chain to regenerate the oxidized cofactor.[20]

To determine the functional activities of both enzyme types in a biosynthetic pathway leading to the production of L-HPG, an *in vivo* complementation approach was designed. As a host, we constructed a mutant from the CDA-producing *S. coelicolor* M1144 in which the gene encoding the second enzyme of the L-HPG biosynthetic pathway, which is required for CDA production, was inactivated. A transposon insertion mutant in *hmO* was created by a double-crossover recombination of the cosmid StE8.1.H04 into *S. coelicolor* strain M1144, resulting in mutant strain LW107 (see Methods for details).

Similar to the phenotype observed by Hojati et al.[4] for an *hmaS*-deletion strain, the resulting *hmO* insertion mutant did not produce CDA detectable in standard plate bioassays[26] (Figure 2A). There was also no trace of detectable CDA when analyzed by UHPLC-MS and compared to M1144 cultures and to a standard of pure CDA-3a (Figure 3A). However, when grown in media containing 1 mM L-HPG, mutant LW107 produced clear zones of inhibition, which may result from restoration of CDA production (Figure 2A). Thus, L-HPG synthesis is the only step in CDA production that is affected in this mutant.

Phylogenetic Analysis Reveals Several Orthologs of hmO and mdlB Genes. Using the amino acid sequences of HmO from *S. coelicolor* (UniProt Q9Z4X8) and MdlB from *Pseudomonas fluorescens* (UniProt Q5EG59) in BLAST searches, putative orthologs of these proteins were identified from the nonredundant NCBI database. Because of their mutual similarity, the BLAST hits of HmO and MdlB were combined into one alignment and in one phylogenetic tree. The evolutionary distances were calculated using the Poisson correction method,[27] and a phylogenetic tree was created using MEGA5[28] (Supporting Information Figure S2). The bacteria harboring the closest homologues of *hmO* all belong to the order Actinomycetales, a group of bacteria known for producing several commercial antibiotics.[29] In contrast, the bacteria that harbor the closest *mdlB* orthologs are from different bacterial orders within the phylum Proteobacteria

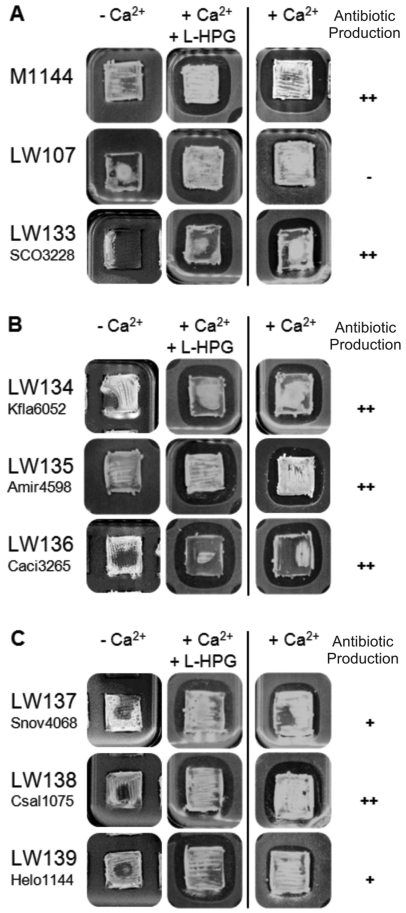

Figure 2. CDA production in *S. coelicolor* M1144 (the parent), LW107 (*hmO*::Tn5), and its complemented strains. CDA bioassays were carried out on SMMS by incubating a square patch of each *S. coelicolor* strains for 30 h at 30 °C and then overlaying them with *B. subtilis* in soft Difco nutrient agar. A clear halo indicates CDA production. (A) M1144: *S. coelicolor* parent containing a wild-type L-HPG operon; LW107: M1144 *hmO::Tn5*; LW133: *hmO* mutant strain complemented with *S. coelicolor hmO*. (B) LW134, LW135, and LW136: LW107 expressing Hmo homologues Kfla6052, Amir4598, Caci3265, respectively. (C) LW137, LW138, and LW139: LW107 complemented with MdlB orthologs Snov4068, Csal1075, and Helo1144, respectively. 30 mM $Ca(NO_3)_2$ (Ca^{2+}) and 1 mM L-HPG were added to the medium when indicated. In the absence of Ca^{2+}, no inhibition zones are observed in any of the strains, as CDA is produced only under calcium induction. The production of CDA is indicated by symbols: (−) No halo; (+) halo smaller than that of LW133; (++) halo similar to that of LW133.

(Supporting Information Figure S2). In order to study the catalytic properties of distantly related homologues, the putative HmO orthologs from *Actinosynnema mirum* (Amir4598; UniProt C6WLN8), *Catenulispora acidiphila* (Caci3265, UniProt C7Q7H9), and *Kribbella flavida* (Kfla6052; UniProt D2PT03) and putative MdlB orthologs from *Chromoholobacter salexigens* (Csal1075; UniProt Q1QYM6), *Halomonas elongata* (Helo1144; UniProt E1V4X8), and *Starkeya novella* (Snov4068; UniProt D7A0L7) (Table I) were selected to test the ability to complement the *hmO* mutant LW107.

Interestingly, while the putative HmO orthologs from *S. coelicolor*, *K. flavida*, and *A. mirum* are composed of 377, 375, and 376 AA, respectively, the enzyme from *C. acidiphila* is 678 amino acids long. The alignment between the different proteins

DOI: 10.1021/sb500368w
ACS Synth. Biol. 2015, 4, 796−807

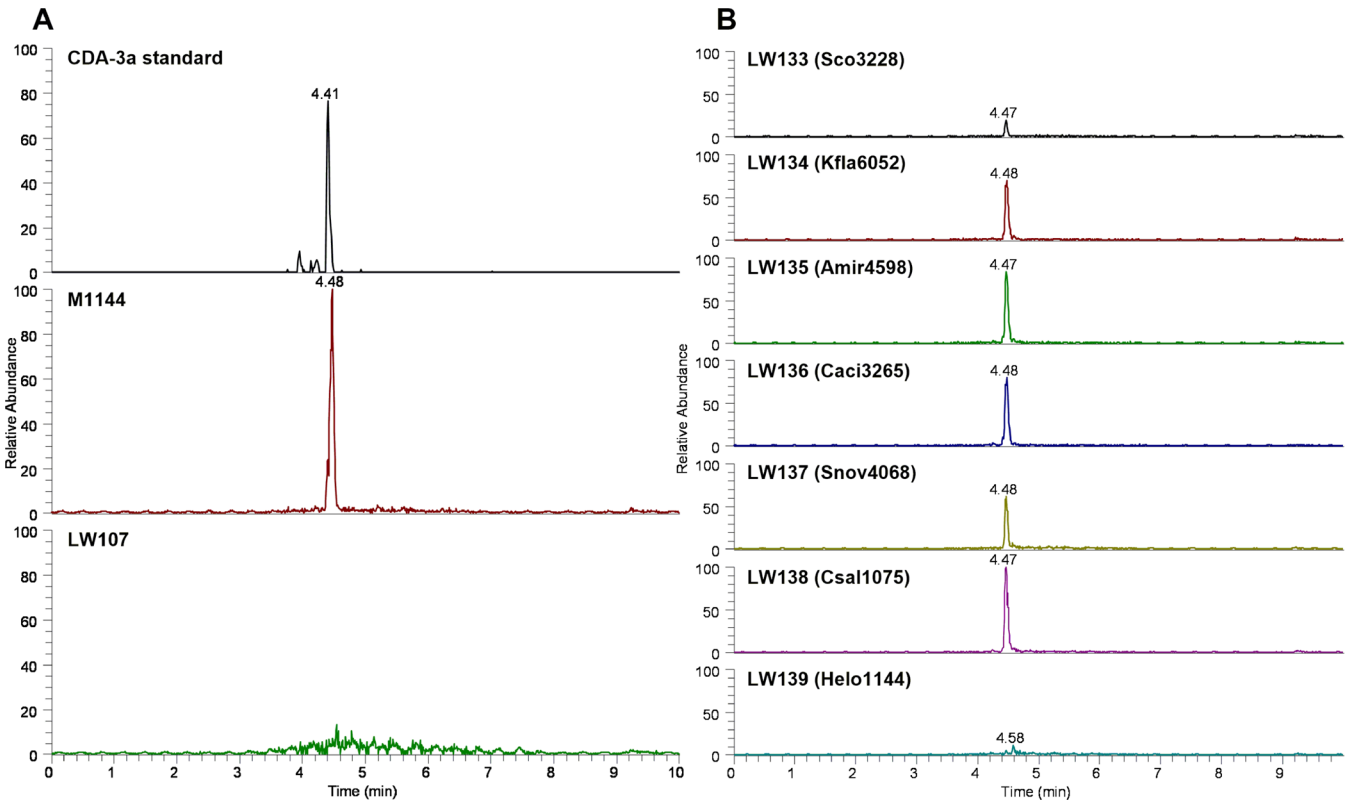

Figure 3. UHPLC-MS analysis of CDA production in *S. coelicolor* M1144 (the parent), LW107 (*hmO*::Tn5), and its complemented strains. Shown are extracted ion chromatograms for the mass range of known CDA variants (m/z 1480−1600). Retention times (t_R) of peaks are shown (min). Data for a sample of pure, previously fully characterized CDA-3a is provided for comparison.[56] (A) CDA-3a pure standard; M1144: *S. coelicolor* parent containing a wild-type L-HPG operon; LW107: M1144 *hmO::Tn5*. (B) LW133: *hmO* mutant strain complemented with *S. coelicolor hmO*; LW134, LW135, and LW136: LW107 expressing HmO homologues Kfla6052, Amir4598, Caci3265, respectively; LW137, LW138, and LW139: LW107 complemented with MdlB orthologs Snov4068, Csal1075 and Helo1144, respectively. Peak heights are displayed relative to the height of LW138 (100% relative abundance). No detectable CDA could be found in LW107, and only a trace, in LW139. The peak with t_R 4.4 min in all of the other samples showed evidence of either CDA-4a or CDA-4b (see Supporting Information for spectra).

Table I. Predicted Function of the Identified Genes[a]

ORF no.[a]	AA[b]	putative function	strain	acc. no.[c]
Caci3265	678	L-HMA oxidase	*Catenulispora acidiphila* DSM 44928	NC013093
Amir4598	376	L-HMA oxidase	*Actinosynnema mirum* DSM 43827	NC013131
Kfla6052	375	L-HMA oxidase	*Kribbella flavida* DSM 17836	NC013729
Sco3228	377	L-HMA oxidase	*Streptomyces coelicolor* M145	NC003888
Csal1075	399	L-mandelate dehydrogenase	*Chromohalobacter salexigens* DSM 3043	NC007963
Helo1144	393	L-mandelate dehydrogenase	*Halomonas elongata* DSM 2581	NC014532
Snov4068	396	L-mandelate dehydrogenase	*Starkeya novella* DSM 506	NC014217

[a]ORF numbers and strain information are from GenBank. [b]Number of amino acid residues. [c]GenBank accesion number.

showed significant sequence similarity of the three first enzymes with the C-terminal part of *C. acidiphila* HmO, whereas the first 276 residues from the latter enzyme are not conserved in the other sequences. However, the N-terminal part of the putative *C. acidiphila* HmO shows homology to bacterial oxoacyl-[acyl-carrier-protein] synthase 3 (Supporting Information Table SI); thus, this HmO is encoded by a chimeric fusion gene.[30]

The dehydrogenase-type hydroxymandelate oxidase MdlB was previously reported to be a membrane-associated protein in *Pseudomonas putida*,[20,31] and an internal segment (residues 177 to 215) was shown experimentally to be responsible for binding to a membrane (Supporting Information Figure S1, red box). Hydropathy profile analysis of this sequence is, however, not consistent with a putative membrane-association domain. This observation together with the low conservation of this region (Supporting Information Figure S1, red box) is seen in the alignment among *P. putida* MdlB, Csal1075, Helo1144, and Snov4068, thus hindering predictions on protein topology.

HmO and MdlB Orthologs Complement the *S. coelicolor* hmO Mutant. Considering that the *hmaS*, *hmO*, and *hpgT* genes comprise a single operon for L-HPG synthesis in *S. coelicolor*,[4] *hmO* insertional inactivation might interfere with transcription and translation of the downstream gene *hpgT*, which encodes an aminotransferase for conversion of 4-hydroxyphenylglyoxylate to L-HPG. To investigate this possibility, CDA biosynthesis was tested in a complemented strain (LW133) that ectopically expresses native *hmO*. This strain was constructed by transforming the *hmO* mutant with the integrative plasmid pTE421 containing the native *S.*

DOI: 10.1021/sb500368w
ACS Synth. Biol. 2015, 4, 796−807

Table II. Plasmids and Cosmids Used and Created in This Study

expression	plasmids/cosmids	description	ref
	pGEM-T Easy	PCR cloning vector	Promega
	pET28b	*E. coli* vector for expression under the control of the T7 promoter	Novagene
	pIJ10257	*permE**, ΦBT1 *attP-int* derived integration vector for conjugal transfer from *E. coli* to *Streptomyces* spp.	44
	pTE399	pGEM-T Easy harboring Kfla6052 from *K. flavida* DSM 17836	this work
	pTE405	pGEM-T Easy harboring Sco3228 from *S. coelicolor* M145	this work
	pTE408	pGEM-T Easy harboring Snov4068 from *S. novella* DSM 506	this work
Kfla6052	pTE412	pIJ10257 harboring Kfla6052 from pTE399	this work
Sco3228	pTE421	pIJ10257 harboring Sco3228 from pTE405	this work
Snov4068	pTE435	pIJ10257 harboring Snov4068 from pTE408	this work
Amir4598	pTE438	pIJ10257 harboring Amir4598 from pTE781	this work
Caci3265	pTE441	pIJ10257 harboring Caci3265 from pTE783	this work
Csal1075	pTE443	pIJ10257 harboring Csal1075 from pTE785	this work
Helo1144	pTE444	pIJ10257 harboring Helo1144 from pTE786	this work
	pTE781	pGEM-T Easy harboring Amir4598 from *A. mirum* DSM 43827	this work
	pTE783	pGEM-T Easy harboring Caci3265 from *C. acidiphila* DSM 44928	this work
	pTE785	pGEM-T Easy harboring Csal1075 from *C. salexigens* DSM 3043	this work
	pTE786	pGEM-T Easy harboring Helo1144 from *H. elongata* DSM 3044	this work
Helo1144	pTE787	pET28b harboring Helo1144 from pTE786	this work
Snov4068	pTE793	pET28b harboring Snov4068 from pTE408	this work
Sco3228	pTE795	pET28b harboring Sco3228 from pTE405	this work
Csal1075	pTE797	pET28b harboring Csal1075 from pTE785	this work
Caci3265	pTE798	pET28b harboring Caci3265 from pTE783	this work
Kfla6052	pTE800	pET28b harboring Kfla6052 from pTE399	this work
Amir4598	pTE803	pET28b harboring Amir4598 from pTE781	this work
	pUZ8002	RP4 derivative, defective *oriT*, supplies a mobilization function for *oriT*-containing plasmids	45
	StE8.1.H04	StE8 *Streptomyces* cosmid Sco3228::Tn5062	54

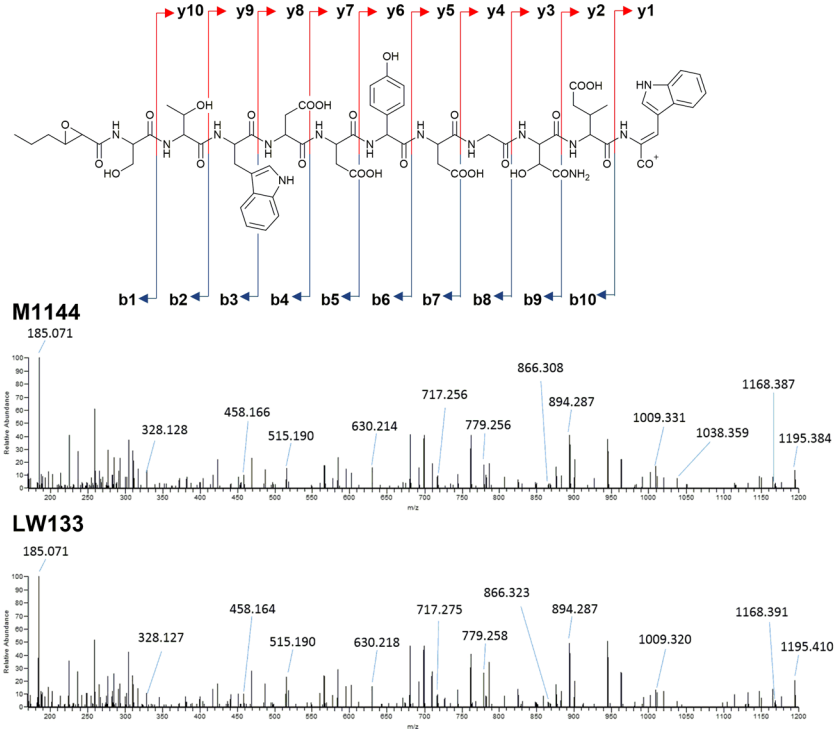

Ion	Calculated	Observed	
		M1144	LW133
y10	1296.444	1296.447	1296.441
y9	1195.396	1195.384	1195.410
y8	1009.317	1009.331	1009.320
y7	894.290	894.287	894.287
y6	779.263	779.256	779.258
y5	630.215	630.214	630.218
y4	515.189	515.190	515.190
y3	458.167	458.166	458.164
y2	328.129	328.128	328.127
y1	185.071	185.071	185.071
b10	1311.465	-	-
b9	1168.407	1168.387	1168.391
b8	1038.369	1038.359	1038.357
b7	981.347	981.339	981.351
b6	866.320	866.308	866.323
b5	717.273	717.256	717.275
b4	602.246	602.243	602.246
b3	487.219	487.217	487.219
b2	301.140	-	301.138
b1	200.092	-	-

Figure 4. MS-MS analysis of CDA-4a produced by *S. coelicolor* M1144 (the parent) and *hmO* (SCO3228) complemented mutant LW133. Shown are selected fragment ions generated from a linearized fragment ion of CDA-4a (structure provided in the figure). Observed fragment ions compare well to calculated values. Most of the fragments shown contain the L-HPG moiety and therefore help to confirm the presence of L-HPG in the complemented mutant.

coelicolor hmO fused to the strong constitutive *ermE** promoter but lacking a downstream copy of *hpgT* (Table II). In biological assays, the resulting complemented mutant showed restored antibiotic activity (Figure 2A, right panel). Correspondingly, UHPLC-MS analysis of this strain showed a peak with a similar retention time as that of a pure standard of CDA-3a and with

DOI: 10.1021/sb500368w
ACS Synth. Biol. 2015, 4, 796−807

an associated mass of 1495.5184, which is consistent with the presence of singly charged CDA-4a (theoretical mass 1495.5284 (−6.6 ppm)) (Figure 3B and Supporting Information Figures S3 and S4). The identity of CDA-4a was further confirmed by tandem MS analysis, where the relevant fragment ions show the presence of L-HPG in both M1144 and complemented mutant LW133 (Figure 4). These results demonstrate that the *hmO*-disrupted mutant LW107 is still capable of expressing a functional aminotransferase from the *hpgT* located downstream of the *hmO*-disrupted region.

A complementation approach was carried out to examine the function of the heterologous hydroxymandelate oxidizing enzymes. For this, we cloned the *hmO* and *mdlB* genes from *A. mirum*, *C. acidiphila*, and *K. flavida* as well as the MdlB orthologs from *C. salexigens*, *H. elongata*, and *S. novella* into the integrative vector pIJ10257, in all cases under control of the *ermE** promoter (Table II). After transforming the *S. coelicolor* *hmO*-defective mutant LW107 with these expression vectors containing *hmO* and *mdlB* genes, the resulting strains were tested for the ability to produce CDA antibiotics by both biological activity assays (Figure 2B,C) and UHPLC-MS (Figure 3B and Supporting Information Figures S3−S5 and Table SIV).

When tested for their biological activity, even in the absence of external addition of 1 mM L-HPG, a clear inhibition halo was visible in all of the samples except LW139 (expressing the *H. elongata* MdlB) (Figure 2B,C). For the latter strain, a very weak halo was observed, barely larger than the HmO mutant strain LW107, suggesting limited CDA complementation. Parent strain M1144 produced similar CDA-inhibition zones when grown on SMMS plates with or without supplement of 1 mM L-HPG (Figure 2A, left and central panels of M1144). Furthermore, the use of higher concentrations of L-HPG (2 to 10 mM) did not significantly increase the inhibition halos (data not shown), indicating that formation of L-HPG is not the rate-limiting step for the production of CDA in the parent strain. On the other hand, for the strains where the inhibition zones were the smallest (those complemented with MdlB orthologs Snov4068 and Helo1144), the inhibition halos increased upon the addition of 1 mM L-HPG (Figure 2C, right panels). The reduced activity with these enzymes may be due to reduced catalytic activity or to impaired expression or stability, in agreement with the membrane-association properties reported for *P. putida* MdlB,[20,31] as discussed below.

In agreement with the biological assay, UHPLC-MS analysis of culture supernatants showed that, except for the Helo1144-expressing LW139, CDA production was restored to similar levels in all of the complemented strains (Figure 3C and Supporting Information Figure S3B; all masses are accurate to <5 ppm) as that seen in the parent strain. Since LW139 extracts showed only a small trace of CDA production (Figure 3B and Supporting Information Figure S3C), high-resolution analysis of this strain was carried out using a Q-Exactive plus mass spectrometer (Thermo Scientific). The analysis data confirmed the production of the major peak corresponding to CDA-4a (Supporting Information Figure S4; mass accuracy of 0.2 ppm). As expected, supernatants from control cultures of the complemented strain LW133 grown in the absence of Ca^{2+} showed no significant levels of CDA (Supporting Information Figure S5).

Unexpectedly, while the majority of CDA produced by the parent strain M1144 was in the form of CDA-4b (the integrated area under the curve of CDA-4b [*m*/*z* 1497] is twice of CDA-4a [*m*/*z* 1495], Supporting Information Figure S4 and Table SIV), in all of the complemented mutants production was seen to shift to mainly CDA-4a. This latter species contains a Z-dehydrotryptophan residue rather than the L-Trp residue at the C-terminus of CDA-4b.[10] However, since the enzyme responsible for oxidation of the C-terminal L-Trp residue has yet to be fully characterized, the reason for this subtle shift is unknown at this time.

All in all, these results indicate that not only the HmO orthologs (Caci3265, Amir4598, and Kfla6052) but also two of the MdlB enzymes (Csal1075 and Snov4068) are able to effectively complement the *hmO* mutant LW107, despite the early evolutionary divergence between Actinobacteria and Proteobacteria.[32]

Expression and Purification of the HmO and MdlB Variants. In order to characterize the *in vitro* properties of the orthologous proteins that showed *in vivo* complementation, they were expressed as N-terminally His-tagged recombinant proteins in *E. coli*. Each of the candidate genes was amplified and cloned into the pET28b(+) expression vector, followed by introduction of the resulting constructs into *E. coli* BL21(DE3). For optimizing the yield of soluble and active proteins, *hmO*-expressing cells were induced in TB medium[33] by adding IPTG, whereas an autoinduction protocol[34] was applied for the MdlB proteins. The His-tagged recombinant proteins were affinity-purified using Ni-NTA columns (Figure 5A and Supporting Information Figure S6), and the identity of the purified proteins was confirmed by western blot analysis using anti-His antibodies (Figure 5B).

The HmO homologues from *A. mirum* (Amir4598), *K. flavida* (Kfla6052), and *S. coelicolor* (Sco3228) yielded ∼50 mg of pure soluble protein per liter of culture. The amount of the purified Sco3228 protein was similar to that obtained by calculating the FMN content (absorbance at 375 or 480 nm),

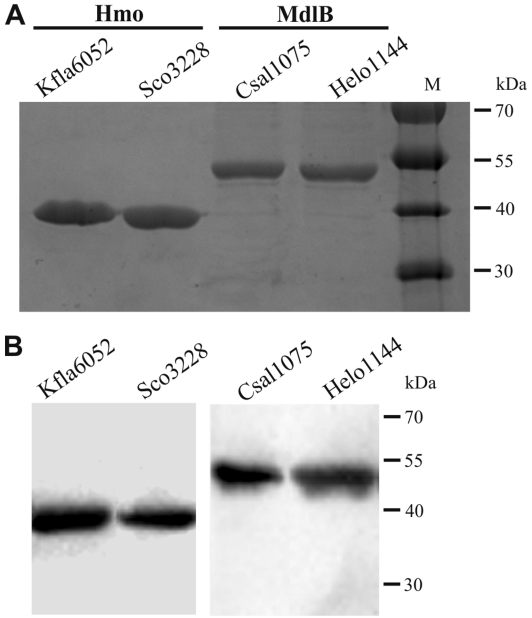

Figure 5. Purification of Hmo and MdlB orthologs. (A) The purified His-tagged proteins, enzymatically characterized, were separated by SDS-PAGE. HmOs Kfla6052 (38.5 kDa) and Sco3228 (38.2 kDa) and MdlBs Csal1075 (44.44 kDa) and Helo1144 (43.78 kDa) were loaded in a single gel. M, molecular weight marker. (B) Western blot of the purified proteins shown in (A), using anti-His antibodies.

DOI: 10.1021/sb500368w
ACS Synth. Biol. 2015, 4, 796−807

Table III. Kinetic Parameters for HmOs and MdlBs with Different Substrates

substrate		DL-HMA			L-mandelate		
protein		k_{cat} (s^{-1})	K_m (mM)	k_{cat}/K_m (s^{-1} mM^{-1})	k_{cat} (s^{-1})	K_m (mM)	k_{cat}/K_m (s^{-1} mM^{-1})
HmO[a]	Sco3228	3.5 ± 0.2	64 ± 4	55.5	1.2 ± 0.1	44 ± 6	26. 3
	Kfla6052	3.27 ± 0.04	96 ± 4	34.1	0.175 ± 0.002	54 ± 5	3.2
MdlB[b]	Csal1075	0.34 ± 0.02	1175 ± 56	0.29	0.995 ± 0.001	177 ± 3	5.61
	Helo1144	1.02 ± 0.01	232 ± 7	4.39	2.77 ± 0.01	234 ± 6	11.9

[a]HmO activities were tested using O_2 as an electron acceptor. [b]MdlB activities were tested using DCPIP [2,6-dichlorophenol-indophenol] as an electron acceptor.

and, accordingly, this protein showed the highest activity. By contrast, as reported for other HmO enzymes,[12,15] the preparations of Kfla6052 and Amir4598 exhibited loss of intrinsic FMN and irreversible inactivation. By adding FMN and glycerol to the purification buffers (Methods), active FMN-containing preparations of Kfla6052 but not of Amir4598 were obtained. For Caci3265, the chimeric HmO from *C. acidiphila*, no expression conditions were found that allowed purification of the recombinant protein. Given the difficulties encountered during isolation of active preparations of Amir4598 and Caci3265, further activity tests were performed only with Sco3228 and Kfla6052 (Figure 5).

Initial attempts to purify the MdlB orthologs failed due to their low expression and solubility. For example, Helo1144 and Csal1075 were purified from autoinduced cultures, but these proteins showed no activity. As rapid inactivation of the *P. putida* MdlB due to irreversible loss of FMN has been reported,[35] modified buffers containing 10 mM β-mercaptoethanol, 1 μM FMN, and glycerol were used for the purification of active enzymes (Figure 5). Both *C. salexigens* Csal1075 and *H. elongata* Helo1144 MdlB homologues were purified in soluble form from *E. coli* extracts using this optimized buffer, thus allowing further characterization of these proteins (Figure 5). In contrast, the unsuccessful efforts to overexpress and purify the His-tagged Snov4068 from *E. coli* together with the low antibacterial activity observed for the *S. coelicolor* strain expressing the MdlB homologue from *S. novella*, Snov4068 (Figure 2C, right panel), suggest low protein solubility and/or stability. It has to be noted, however, that since none of the orthologous genes were codon-optimized for expression in *E. coli* or *S. coelicolor*, nor was their GC content modified, differences in the expression levels between the HmO and MdlB proteins could also affect their relative activities and purification yields.

Enzyme Activity of the HmO Orthologs. The oxidation of HMA catalyzed by HmO was assayed using racemic substrate and monitoring the production of 4-hydroxyphenylglyoxylate at 340 nm. As expected, product formation was observed with the *K. flavida* and *S. coelicolor* HmO enzymes, confirming the activity detected in the *in vivo* complementation experiments. Stereoselectivity of the enzymes was determined by separately testing the oxidation of L- or D-mandelate at 252 nm. In agreement with previous reports on the corresponding enzymes from *S. coelicolor* and *Amycolatopsis orientalis*,[4,12,16,23] the purified HmOs converted the L-mandelate to phenylglyoxylate, but not the D-enantiomer. These results, together with previous reports on HmO activities, indicate a L-stereospecificity for these enzymes. This could not be tested for HMA, as the enantiomerically pure compound is not commercially available.

The kinetic parameters obtained for the two HmOs are summarized in Table III. The enzymes have a relaxed specificity and convert both hydroxylated and nonhydroxylated forms of the substrates, in agreement with earlier observations on enzymes of the HPG biosynthetic pathway.[4,23] In fact, considering that only the L-enantiomer of the racemic DL-HMA is expected to be oxidized by Kfla6052 and Sco3228, both enzymes showed similar affinities for HMA and mandelate. However, it is noteworthy that the *K. flavida* HmO exhibited a significant preference for the hydroxylated substrate, as clear from the 20-fold higher turnover number (k_{cat}) for this compound as compared to that for mandelic acid (Table III). This indicates that Kfla6052 has a higher substrate specificity than Sco3228, whose k_{cat} with L-mandelate is 3-fold lower than that with DL-HMA. Furthermore, the catalytic efficiency of *S. coelicolor* HmO with HMA is of the same order of magnitude as with mandelate (55.5 and 26.3 s^{-1} mM^{-1}, respectively), whereas for Kfla6052, a 10-fold lower k_{cat}/K_m value was obtained with the nonhydroxylated substrate (Table III). This high catalytic performance obtained *in vitro* for the *K. flavida* protein is consistent with the fully complemented CDA activity displayed by the *S. coelicolor* mutant LW107 expressing Kfla6052 (Figure 2B). The efficient oxidation of L-mandelate exhibited by both Kfla6052 and Sco3228 (although lower than that of DL-HMA) could suggest flexibility in the active sites and the ligand-binding pockets of these oxidases.

In summary, the outstanding expression levels and the high stability of Sco3228 and Kfla6052, in combination with their ability to oxidize different substrates, indicate that these two oxidases could be excellent candidates for future application in precursor supply engineering for NRPs.

Catalytic Activity of the MdlB Orthologs. For the characterization of the MdlB-related enzymes, Csal1075 and Helo1144, the oxidation of DL-HMA was analyzed in the presence of different electron acceptors, including oxygen, which was tested using a protocol similar to that for HmO. As expected for dehydrogenase members of the α-hydroxyacid-oxidizing enzyme family,[20,31] Csal1075 and Helo1144 did not use molecular oxygen as an electron acceptor. Activity was neither detected in the presence of NAD^+ nor in the presence of $NADP^+$, in agreement with previous reports in which D- but not L-mandelate dehydrogenases are NAD^+-dependent enzymes.[36] The fact that *C. salexigens* and *H. elongate* MdlBs were unable to use NAD^+, $NADP^+$, or oxygen is consistent with the assumption that ubiquinone or another membrane-bound electron carrier acts as the physiological electron acceptor in the oxidative reactions catalyzed by L-mandelate dehydrogenases.[20,21] Multiple sequence alignments show that the residue corresponding to Gly81 in the *P. putida* MdlB is also a Gly in the three dehydrogenases, whereas it is an Ala in the oxidases (Supplorting Information Figure S1, green arrows). These observations are consistent with results of Dewanti et al.,[37] who demonstrated that a Gly81 to Ala mutation in *P. putida* MdlB enhances the reactivity with oxygen.

DOI: 10.1021/sb500368w
ACS Synth. Biol. 2015, 4, 796−807

Dehydrogenase activities of Csal1075 and Helo1144 were assayed by measuring the reduction of the artificial electron acceptor 2,6-dichloroindophenol (DCPIP) at 600 nm. Lehoux and Mitra[35] and Xu and Mitra[20] showed that activity of *P. putida* MdlB is obtained when phenazine methosulfate is present as an artificial electron acceptor. However, in the case of *C. salexigens* and *H. elongata* MdlBs, under similar conditions as those previously reported, substrate-independent reduction of DCPIP was observed, probably due to the presence of reduced phenazine methosulfate that was acting as electron donor, thus precluding further analysis. Therefore, subsequent experiments with these enzymes were performed in the absence of phenazine methosulfate, conditions in which the DCPIP becomes the second substrate of the assay.[20]

As shown in Table III, both enzymes were able to oxidize not only L-mandelate but also the hydroxylated compound, as previously shown for other MdlB orthologs.[14−16] However, both *C. salexigens* and *H. elongata* MdlBs oxidize L-mandelate more efficiently than DL-HMA (20- and 3-fold higher k_{cat}/K_m for Csal1075 and Helo1144, respectively) (Table III). This is in agreement with the role of these enzymes in the utilization of L-mandelate as the sole source of carbon and energy.[20] The enzyme Helo1144 was 10 times more efficient in oxidizing DL-HMA than the *C. salexigens* MdlB (k_{cat}/K_m of 4.39 and 0.29 s^{-1} mM^{-1}, respectively) (Table III). However, the *S. coelicolor* mutant expressing the *H. elongata* ortholog displays a lower CDA production than the Csal1075-expressing strain (Figures 2C and 3B). The difference between results obtained *in vivo* and *in vitro* for *H. elongata* MdlB suggests impaired expression or stability of this protein in *S. coelicolor*. Remarkably, even when the affinity of Csal1075 for DL-HMA is 10 times lower than for the nonhydroxylated compound (K_m of 1175 and 177 μM, respectively) and the k_{cat} is only ∼30% of the value for L-mandelate (Table III), its activity is sufficient to support CDA synthesis in *S. coelicolor* LW107 (Figures 2C and 3B). Neither Csal1075 nor Helo1144 showed activity toward D-mandelate (data not shown), indicating L-stereospecificity. Activity was also not detected when lactate or glycolate were tested as substrate, which could indicate that small alcohols are not good substrates.

In conclusion, these results demonstrate that antibiotic building blocks can be provided by enzymes with different metabolic roles that have not been optimized for a specific activity. Once their catalytic performance is improved, the use of enzymes from unrelated pathways for the fermentative production of bioactive compounds could be significantly advantageous to avoid potentially dangerous reaction products (e.g., H_2O_2 produced by HmOs) as well as to choose from different cofactor requirements or expression features of the enzymes.

Future Perspectives. The continued emergence of antibiotic-resistant strains and the increasing failure of antibacterials to pass noninferiority trials have raised the need for alternative therapeutic options.[1,2] The development and overproduction of novel bioactive secondary metabolites has been recently explored by reprogramming antibiotic biosynthetic pathways using a combination of increasingly powerful genetic tools and the wealth of new sequence information, i.e., by use of synthetic biology.[1,2,22] This study demonstrates that the catabolic enzymes involved in unrelated metabolic pathways can be used as plug-and-play parts in an engineered biosynthetic pathway, thus broadening the possibilities for industrial-scale production and design of novel antimicrobial/therapeutic compounds by synthetic biology.

METHODS

Bacterial Strains, Plasmids, and Growth Conditions. Bacterial strains used in this work are described in Table IV.

Table IV. Bacterial Strains Used and Created in This Study

strains	description	ref
B. subtilis		
ATCC 6633	wild type	47
E. coli		
BL21(DE3)	F⁻ *ompT gal dcm lon hsdS*$_B$(r_B^- m_B^-) *λ*(DE3 [*lacI lac*UV5-T7 gene 1 *ind*1 *sam*7 *nin*5])	38
ET12567	methylation-deficient, *dam-13::Tn9 dcm-6 hsdM hsdR recF143 zjj201::Tn10 galK2 galT22 ara-14 lacY1 xyl-5 leuB6 thi-1 ton*A31 *rpsL*136 *hisG*4 *tsx*-78 *mtl-1 gln V*44 F⁻	40
K12 JM101	general cloning strain, F¢ *traD36 proA*$^+$*B*$^+$ *lacI*^{q} Δ*(lacZ)M*15/ Δ*(lac-proAB) gln V thi*	39
S. coelicolor		
LW107	M1144 Sco3228::*Tn*5062	this work
LW133	LW107::pTE421	this work
LW134	LW107::pTE412	this work
LW135	LW107::pTE438	this work
LW136	LW107::pTE441	this work
LW137	LW107::pTE435	this work
LW138	LW107::pTE443	this work
LW139	LW107::pTE444	this work
M1144	M145 derivative, Δ*act* Δ*red* Δ*cpk*	42
M145	wild type, *S. coelicolor* A3(2) derivative SCP1⁻ SCP2⁻	41

Escherichia coli strains BL21(DE3),[38] JM101,[39] and ET12567[40] were transformed as described by Sambrook et al.[39] *S. coelicolor* A3(2) strains M145,[41] M1144,[42] and LW107 (this work) were manipulated as described by Kieser et al.[43] Vectors used were pGEM-T Easy (Promega), pET28b (Novagen, Madison, WI), and pIJ10257.[44] MS agar[43] was used to grow sporulating cultures of *Streptomyces* strains and was supplemented with 10 mM $MgCl_2$ to carry out conjugations between *Streptomyces* and *E. coli* ET12567 containing the pUZ8002 mobilization vector.[45] LB broth (Sigma-Aldrich) and TSB[43] were used to grow *E. coli* and *Streptomyces* for genomic DNA and plasmid isolation, respectively. Liquid cultures for LC-MS analysis were grown in 50 mL of SV2 medium in siliconized 250 mL flasks containing coiled springs. SV2 contains 15 g/L soy peptone, 15 g/L D-glucose, 15 g/L glycerol, 3 g/L NaCl, and, where required, 1 g/L $CaCO_3$.[4] Spore inoculum was approximately 2×10^8 sfu per 50 mL flask. After 3 days growth at 30 °C, shaking at 250 rpm, cultures were centrifuged at 3200*g* for 40 min in a swing out rotor to remove the cell debris. The supernatant was acidified to pH 2 and spun again for 40 min at 3200*g*. The acidified supernatants were applied to 12 mL C18 Bond Elut columns (Mega BE-C18, Agilent). The Bond Elut columns were washed with 2 × 10 mL of water, followed by an eluting wash of 2 × 10 mL with 20, 50, and then 100% MeOH (HPLC grade). Samples were vacuum-dried and resuspended in 100 μL of acetonitrile (ACN). CDA was always detected in the 100% elution fractions (by initial HPLC analysis, compared to a CDA standard). The semipurified samples were then analyzed by UHPLC-MS. For the biological assays to determine antibacterial activity, SMMS plates supplemented with 30 mM $Ca(NO_3)_2$ were inoculated with a 4×10^7 CFU spore solution

DOI: 10.1021/sb500368w
ACS Synth. Biol. 2015, 4, 796−807

of *Streptomyces* A3(2) strains in 2.5 cm^2 patches. SMMS is the agar version (2%, w/v) of SMM as reported by Takano et al.,[46] but it lacks $(NH_4)_2SO_4$ and PEG. After 30 h incubation at 30 °C, the plates were overlaid with soft Difco nutrient agar containing a 1000-fold dilution of an overnight culture in liquid LB medium of *B. subtilis* ATCC 6633[47] as an indicator strain. Plates were examined after an additional 16 h of growth at 30 °C for CDA-inhibition halos.

Identification of HmO and MdlB Orthologs. In order to identify genes that could be used in the complementation studies, BLAST searches were performed against the nonredundant protein sequence database, the Protein Data Bank[48] and the SwissProt database,[49] using HmO from *S. coelicolor* A3(2) [UniProt Q9Z4X8] and (*S*)-hydroxymandelate dehydrogenase MdlB from *P. fluorescens* EBC191[50] [UniProt Q5EG59] as queries. The amino acid sequences of the 100 best hits from the NCBI database of nonredundant protein sequences and the most significant hits from SwissProt and PDB were aligned using MUSCLE.[51] Phylogenetic trees were constructed from these alignments using the neighbor-joining method[52] with 100 bootstrap replication tests.[53]

Genomic DNA of the bacterial strains harboring putative orthologs of *hmO* and *mdlB* (Table I) was acquired from DSMZ (http://www.dsmz.de/); genomic DNA from *S. coelicolor* M145 was isolated from an overnight culture. DNA was amplified and sequenced using primers annealing outside the annotated gene sequence on the NCBI database to ensure that the correct start and stop codons are present (Supporting Information Table SII).

Construction of the *S. coelicolor* L-HPG Pathway Mutant. Transposon cosmid StE8.1.H04[54] carrying a Tn5062 insertion in *S. coelicolor hmO* (Ordered locus name SCO3228) (Table II), was introduced into *S. coelicolor* M1144 by conjugation using the methylation-deficient *E. coli* ET12567/pUZ8002 as a donor as described by Kieser et al.[43] After two rounds of sporulation, apramycin-resistant and kanamycin-sensitive double-crossover mutants were selected and confirmed by PCR, creating the *hmO* insertional inactivation mutant LW107 *hmO*::Tn5062 (Table IV).

Cloning of the Orthologous Genes into pIJ10257 and pET28(+). Once the DNA sequences of the selected genes from *A. mirum*, *C. acidiphila*, *C. salexigens*, *H. elongata*, *K. flavida*, *S. novella*, and *S. coelicolor* were confirmed, the genes were amplified from genomic DNA with *Taq* polymerase using the cloning primers listed in Table SIII (Supporting Information). The PCR products were cloned in the linear pGEM-T Easy vector (Promega), and the resulting cloned sequences were confirmed by sequencing. The created constructs (Table II) were digested with the restriction enzymes corresponding to the amplified recognition sequence (Supporting Information Table SIII) and subcloned in the integrative pIJ10257 *Streptomyces* vector and in the replicative pET28b(+) *E. coli* vector (Table II).

Complementation of *S. coelicolor* LW107 with hmO and mdlB Orthologous Genes. Using *E. coli* ET12567/pUZ8002 as a donor, constructs pTE412, pTE421, pTE435, pTE438, pTE441, pTE443, and pTE444 (Table II) were introduced into LW107 by conjugation as described by Kieser et al.,[43] creating strains LW134, LW133, LW137, LW135, LW136, LW138, and LW139, respectively (Table IV).

Purification of the N-Terminally His-Tagged Proteins. To overexpress and purify the His-tagged versions of the different proteins, *E. coli* strain BL21(DE3) (Table IV) was transformed with plasmids pTE787, pTE793, pTE795, pTE797, pTE798, pTE800, and pTE803. These are pET28b-(+) derivatives harboring a putative *hmO* or *mdlB* gene (Table II). Amir4598, Kfla6052, and Sco3228 expressing *E. coli* (Table II) were cultured in 100 mL of TB medium,[33] grown at 37 °C until OD_{600nm} = 0.6, and then induced with 0.05 mM IPTG for 16 h at 24 °C. Cell pellets were collected by centrifugation (3200*g*, 10 min, 4 °C) and washed with 10 mL of 50 mM Tris-HCl, pH 7.5. Cell disruption was carried out by sonication (15 s × 10) in 2−3 mL of lysis buffer (50 mM NaH_2PO_4, 300 mM NaCl, and 10 mM imidazole, pH 8.0). After centrifugation at 12 000*g* for 10 min, the supernatant was collected and purified by using affinity binding on Ni-NTA resin (Sigma) as described by the manufacturer. Wash and elution buffers contained 50 mM NaH_2PO_4, 300 mM NaCl, and 20 mM imidazole or 50 mM NaH_2PO_4, 250 mM imidazole, and 35% (w/v) glycerol, respectively. For Kfla6052, 1 mM FMN and 10% (w/v) glycerol were added to lysis and wash buffers, whereas the elution buffer additionally contained 1 mM FMN.

Csal1075 and Helo1144-expressing *E. coli* (Table II) were grown in 200 mL of autoinduction medium[34] at 37 °C until OD_{600nm} = 0.6 and were then shifted to 24 °C for 16 h. These two proteins and HmO Kfla6052 were purified as described above using buffers containing 50 mM NaH_2PO_4, 300 mM NaCl, 1 mM FMN, and 10 mM β-mercaptoethanol, pH 8.0. Additionally, each buffer contained the following: lysis buffer (10% (w/v) glycerol and 10 mM imidazole); wash buffer (10% (w/v) glycerol and 20 mM imidazole, pH 8.0); and elution buffer (35% (w/v) glycerol and 250 mM imidazole, pH 8.0).

Purified proteins were quantified by Bradford assay (Bio-Rad protein kit, Bio-Rad Lab. GmbH, Germany), with bovine serum albumin as a standard, as described by the manufacturer.

Western Blot Analysis. For detection of His-tagged proteins, samples containing 20 μg of proteins were boiled in the presence of loading buffer and separated on a 12% SDS-polyacrylamide gel, and proteins were transferred to Hybond-P PVDF membrane (Amersham Biosciences, Piscataway, NJ) as described by the manufacturer. For protein detection, a 1:1000 dilution of mouse monoclonal anti-His antibody (R&D Systems) was applied, followed by a 1:3000 dilution of alkaline phosphatase-labeled goat anti-mouse antibody. Signals were detected with CDP-Star (Tropix-ABI).

Enzyme Activity Determinations. The enzyme characterization of the different proteins was analyzed by a spectrophotometer using 96-well Microplates and a SpectraMax Plus 384 plate reader (Molecular Devices). For each concentration of substrate, reactions were conducted in triplicate. For all experiments, a total volume of 200 μL was used, and control assays were performed using an assay mixture without protein to correct for nonspecific reactions. The molar absorbances of 2,6-dichloroindophenol (DCPIP) (600 nm, 21 600 M^{-1} cm^{-1}) and 4-hydroxyphenylglyoxylate (340 nm, 3510 M^{-1} cm^{-1}) were used to calculate the enzyme activities as described by Xu and Mitra and Müller et al.[20,23]

Activity of MdlB toward DL-4-hydroxymandelate and L-mandelate was determined using 2,6-dichlorophenol-indophenol (DCPIP) as the electron acceptor. Assays were performed at 28 °C in 0.1 M phosphate buffer, pH 7.5, 3 μM FMN, 100 μM DCPIP, and 1 mg/mL BSA. The reaction was started by adding 20 μL of DL-HMA or D- or L-mandelate in different concentrations (0.20−20 mM) and was monitored at 600 nm, which detects reduction of DCPIP.[20]

DOI: 10.1021/sb500368w
ACS Synth. Biol. 2015, 4, 796−807

The activity assays of HmO toward DL-4-hydroxymandelate were carried out as described previously:[15,23] 10 μL of a protein preparation (2−10 μg) was incubated with 100 mM potassium phosphate buffer, pH 7.5, 3 μM FMN, and 20 mg L^{-1} catalase. The reaction was started by adding 20 μL of DL-HMA in different concentrations (0.20−20 mM). The oxidation of 4-hydroxymandelate was monitored spectrophotometrically at 340 nm.

The wavelength for monitoring HmO activity toward L-mandelate was determined by scanning from 200 to 750 nm using a reaction mixture containing 100 mM potassium phosphate buffer, pH 7.5, 3 μM FMN, 20 mg L^{-1} catalase, and 5 μL of purified Sco3228. The absorption peak at 252 nm was chosen, in agreement with previous reports.[55] The extinction coefficient obtained for the L-mandelate at 252 nm was 0.132 mM^{-1} cm^{-1}.

HmO activities using L-mandelate as substrate were characterized using a reaction mixture containing 100 mM potassium phosphate buffer, pH 7.5, 3 μM FMN, 20 mg L^{-1} catalase, and 10 μL of purified protein (2−10 μg). The reaction was started by the addition of 20 μL of L- or D-mandelate in different concentrations (0.2−20 mM). The oxidation of mandelate was monitored spectrophotometrically at 252 nm using Microtest 96-well (clear plates UV−vis transparent film bottom) with a final volume of 200 μL.

UHPLC-MS Analysis of CDA Production. Samples prepared from the SV2 culture supernatants were analyzed using a Waters Acquity UPLC system fitted with a Waters C18 BEH column (100 mm × 2.1 mm, 1.7 μm) using a flow rate of 300 μL min^{-1}. CDAs were eluted using the following gradient: 0−6 min, 5−70% B; 6−7 min, 70−95% B; 7−8 min, 95% B; 8−9 min, 95−5% B; and 9−10 min, 5% B; where A was 0.1% formic acid in water and B was 0.1% formic acid in ACN. Eluent from the HPLC was analyzed by an LTQ Orbitrap XL mass spectrometer (Thermo Scientific) at the Michael Barber Centre, University of Manchester. MS acquisition was carried out at 30 000 resolution in the 200−2000 m/z range. The source voltage was set to 4.2 V, and the capillary ion transfer tube temperature was set at 200 °C.

Further analysis of the LW139 mutant was carried out on a Thermo Q-Exactive Plus hybrid mass spectrometer operated in positive ionization mode coupled to a Thermo-Dionex Ultimate 3000 LC system. Chromatographic separations were performed on a 100 mm Thermo Accucore 2.1 μm C_{18} column at a solvent flow-rate of 400 μL min^{-1}. During the profiling analysis, the column was eluted with 0.1% formic acid in water (A) and 0.1% formic acid in ACN (B). Solvent composition during gradient elution was as follows: 0−2 min, 5% (B); 2−17 min, 5−95% B; 17−20 min, 95%, before returning to 5% (B) and holding for a further 2.5 min for column equilibration. All samples were maintained at 4 °C while the column was maintained at 50 °C within the autosampler oven. MS acquisition was carried out at 70 000 resolution fwhm in continuum mode and was run at 1 μ-scan per 400 ms in the 200−3000 m/z range. The HESI source voltage was set to 4.2 V, and the capillary ion transfer tube temperature was set at 320 °C. All systems were operated using Thermo Xcalibur software, version 3.0.

■ ASSOCIATED CONTENT

Supporting Information

Table SI: Description of the Blast hits of the N-terminal part of Caci3265. Tables SII and SIII: Lists of the primers used in this article. Table SIV: Comparison of CDA-4A production between M1144 and LW139. Figure S1: Alignment between the *S. coelicolor* HmO and L-mandelate dehydrogenases (MdlB) proteins from different bacteria. Figure S2: Phylogenetic tree of the HmO and MdlB orthologs. Figures S3−S5: UHPLC-MS and tandem-MS analysis of the CDA cultures. Figure S6: Purification fractions of the proteins. This material is available free of charge via the Internet at http://pubs.acs.org.

■ AUTHOR INFORMATION

Corresponding Author

*E-mail: eriko.takano@manchester.ac.uk.

Present Addresses

▽(V.D.) Max Planck Institute of Molecular Cell Biology and Genetics, Pfotenhauerstr 108, 01307 Dresden, Germany.

◆(M.L.) Department of Polymer Chemistry & Bioengineering, Zernike Institute for Advanced Materials, University of Groningen, NL-9747 AG Groningen, The Netherlands.

¶(M.H.M.) Bioinformatics Group, Wageningen University, Droevendaalsesteeg 1, 6708 PB Wageningen, The Netherlands.

□(E.T.) Manchester Synthetic Biology Research Center (SYNBIOCHEM), Manchester Institute of Biotechnology, School of Life Sciences, University of Manchester, 131 Princess Street, Manchester, M1 7DN, United Kingdom.

Author Contributions

V.D. and E.T. designed the work; V.D., M.W., and N.J.W.R. analyzed the work; V.D., M.L., S.T., H.P., M.W., N.J.W.R., and M.H.M. conducted the work; V.D., D.B.J., J.M., R.G., and E.T. edited the manuscript; R.B., U.M., D.B.J., and E.T. supervised the work.

Notes

The authors declare the following competing financial interest(s): R.B. and U.M. are employed by DSM. Some of DSM's products are nonribosomal peptides.

■ ACKNOWLEDGMENTS

We thank Rainer Breitling for critically reading the manuscript. V.D. and M.L. were funded by the BE-Basic program under grant no. FS 02.002. M.H.M. was funded by the Dutch Technology Foundation STW, which is the applied science division of NWO and the Technology Program of the Ministry of Economic Affairs (STW 10463). We would also like to acknowledge BBSRC, EPSRC funded Manchester SYNBIO-CHEM (BB/M017702/1).

■ ABBREVIATIONS

AA, amino acids; CDA, calcium-dependent antibiotics; DCPIP, 2,6-dichlorophenol-indophenol; L-HPG, L-4-hydroxyphenylglycine; HMA, hydroxymandelate; HPP, 4-hydroxyphenylpyruvate; HPGL, 4-hydroxyphenylglyoxylate; NRP, nonribosomal peptides

■ REFERENCES

(1) Medema, M. H., Breitling, R., Bovenberg, R., and Takano, E. (2011) Exploiting plug-and-play synthetic biology for drug discovery and production in microorganisms. *Nat. Rev. Microbiol. 9*, 131−137.

(2) Frasch, H.-J., Medema, M. H., Takano, E., and Breitling, R. (2013) Design-based re-engineering of biosynthetic gene clusters: plug-and-play in practice. *Curr. Opin. Biotechnol. 24*, 1−7.

(3) Strieker, M., Tanović, A., and Marahiel, M. A. (2010) Nonribosomal peptide synthetases: structures and dynamics. *Curr. Opin. Struct. Biol. 20*, 234−240.

DOI: 10.1021/sb500368w
ACS Synth. Biol. 2015, 4, 796−807

(4) Hojati, Z., Milne, C., Harvey, B., Gordon, L., Borg, M., Flett, F., Wilkinson, B., Sidebottom, P. J., Rudd, B. A. M., Hayes, M. A., Smith, C. P., and Micklefield, J. (2002) Structure, biosynthetic origin, and engineered biosynthesis of calcium-dependent antibiotics from *Streptomyces coelicolor*. *Chem. Biol. 9*, 1175−1187.
(5) Kempter, C., Kaiser, D., Haag, S., Nicholson, G., Gnau, V., Walk, T., Gierling, K. H., Decker, H., Zähner, H., Jung, G., and Metzger, J. W. (1997) CDA: calcium-dependent peptide antibiotics from *Streptomyces coelicolor* A3(2) containing unusual residues. *Angew. Chem., Int. Ed. Engl. 36*, 498−501.
(6) Steenbergen, J. N., Alder, J., Thorne, G. M., and Tally, F. P. (2005) Daptomycin: a lipopeptide antibiotic for the treatment of serious Gram-positive infections. *J. Antimicrob. Chemother. 55*, 283−288.
(7) Samel, S. A., Marahiel, M. A., and Essen, L.-O. (2008) How to tailor non-ribosomal peptide products-new clues about the structures and mechanisms of modifying enzymes. *Mol. BioSyst. 4*, 387−393.
(8) Neary, J. M., Powell, A., Gordon, L., Milne, C., Flett, F., Wilkinson, B., Smith, C. P., and Micklefield, J. (2007) An asparagine oxygenase (AsnO) and a 3-hydroxyasparaginyl phosphotransferase (HasP) are involved in the biosynthesis of calcium-dependent lipopeptide antibiotics. *Microbiology 153*, 768−776.
(9) Milne, C., Powell, A., Jim, J., Al Nakeeb, M., Smith, C. P., and Micklefield, J. (2006) Biosynthesis of the (2*S*,3*R*)-3-methyl glutamate residue of nonribosomal lipopeptides. *J. Am. Chem. Soc. 128*, 11250−11259.
(10) Amir-Heidari, B., and Micklefield, J. (2007) NMR confirmation that tryptophan dehydrogenation occurs with syn stereochemistry during the biosynthesis of CDA in *Streptomyces coelicolor*. *J. Org. Chem. 72*, 8950−8953.
(11) Sheldrick, G. M., Jones, P. G., Kennard, O., Williams, D. H., and Smith, G. A. (1978) Structure of vancomycin and its complex with acetyl-D-alanyl-D-alanine. *Nature 271*, 223−225.
(12) Hubbard, B. K., Thomas, M. G., and Walsh, C. T. (2000) Biosynthesis of L-*p*-hydroxyphenylglycine, a non-proteinogenic amino acid constituent of peptide antibiotics. *Chem. Biol. 7*, 931−942.
(13) Choroba, O. W., Williams, D. H., and Spencer, J. B. (2000) Biosynthesis of the vancomycin group of antibiotics: involvement of an unusual dioxygenase in the pathway to (*S*)-4-hydroxyphenylglycine. *J. Am. Chem. Soc. 122*, 5389−5390.
(14) Gunsior, M., Breazeale, S. D., Lind, A. J., Ravel, J., Janc, J. W., and Townsend, C. A. (2004) The biosynthetic gene cluster for a monocyclic beta-lactam antibiotic, nocardicin A. *Chem. Biol. 11*, 927−938.
(15) Kastner, S., Müller, S., Natesan, L., König, G. M., Guthke, R., and Nett, M. (2012) 4-Hydroxyphenylglycine biosynthesis in *Herpetosiphon aurantiacus*: a case of gene duplication and catalytic divergence. *Arch. Microbiol. 194*, 557−566.
(16) Li, T. L., Choroba, O. W., Charles, E. H., Sandercock, A. M., Williams, D. H., and Spencer, J. B. (2001) Characterisation of a hydroxymandelate oxidase involved in the biosynthesis of two unusual amino acids occurring in the vancomycin group of antibiotics. *Chem. Commun. 18*, 1752−1753.
(17) Gunter, S. E. (1953) The enzymatic oxidation of *p*-hydroxymandelic acid to p-hydroxybenzoic acid. *J. Bacteriol. 66*, 341−346.
(18) Hegeman, G. D. (1966) Synthesis of the enzymes of the mandelate pathway by *Pseudomonas putida*. I. Synthesis of enzymes by the wild type. *J. Bacteriol. 91*, 1140−1154.
(19) Smékal, O., Reid, G. A. ., and Chapman, S. K. (1994) Substrate analogues as probes of the catalytic mechanism of L-mandelate dehydrogenase from *Rhodotorula graminis*. *Biochem. J. 297*, 247−252.
(20) Xu, Y., and Mitra, B. (1999) A highly active, soluble mutant of the membrane-associated (*S*)-mandelate dehydrogenase from *Pseudomonas putida*. *Biochemistry 38*, 12367−12376.
(21) Lehoux, I. E., and Mitra, B. (2000) Role of arginine 277 in (*S*)-mandelate dehydrogenase from *Pseudomonas putida* in substrate binding and transition state stabilization. *Biochemistry 39*, 10055−10565.
(22) Baltz, R. H. (2014) Combinatorial biosynthesis of cyclic lipopeptide antibiotics: a model for synthetic biology to accelerate the evolution of secondary metabolite biosynthetic pathways. *ACS Synth. Biol. 3*, 748−758.
(23) Müller, U., van Assema, F., Gunsior, M., Orf, S., Kremer, S., Schipper, D., Wagemans, A., Townsend, C. A., Sonke, T., Bovenberg, R., and Wubbolts, M. (2006) Metabolic engineering of the *E. coli* L-phenylalanine pathway for the production of D-phenylglycine (D-Phg). *Metab. Eng. 8*, 196−208.
(24) Tsou, A. Y., Ransom, S. C., Gerlt, J. A., Buechter, D. D., Babbitt, P. C., and Kenyon, G. L. (1990) Mandelate pathway of *Pseudomonas putida*: sequence relationships involving mandelate racemase, (*S*)-mandelate dehydrogenase, and benzoylformate decarboxylase and expression of benzoylformate decarboxylase in *Escherichia coli*. *Biochemistry 29*, 9856−9862.
(25) Sukumar, N., Dewanti, A. R., Mitra, B., and Mathews, F. S. (2004) High resolution structures of an oxidized and reduced flavoprotein. The water switch in a soluble form of (*S*)-mandelate dehydrogenase. *J. Biol. Chem. 279*, 3749−3757.
(26) Chong, P. P., Podmore, S. M., Kieser, H. M., Redenba, M., Hopwood, D. A., and Smith, C. P. (1998) Physical identification of a chromosomal locus encoding biosynthetic genes for the lipopeptide calcium-dependent antibiotic (CDA) of *Streptomyces coelicolor* A3(2). *Microbiology 144*, 193−199.
(27) Zuckerkandl, E., and Pauling, L. (1965) Evolutionary divergence and convergence in proteins, in *Evolving Genes and Proteins* (Bryson, V., and Vogel, H. J., Eds.) pp 97−166, Academic Press, New York.
(28) Tamura, K., Peterson, D., Peterson, N., Stecher, G., Nei, M., and Kumar, S. (2011) MEGA5: molecular evolutionary genetics analysis using maximum likelihood, evolutionary distance, and maximum parsimony methods. *Mol. Biol. Evol. 28*, 2731−2739.
(29) Weber, T., Welzel, K., Pelzer, S., Vente, A., and Wohllebena, W. (2003) Exploiting the genetic potential of polyketide producing streptomycetes. *J. Biotechnol. 106*, 221−232.
(30) Kaessmann, H. (2010) Origins, evolution, and phenotypic impact of new genes. *Genome Res. 20*, 1313−1326.
(31) Sukumar, N., Xu, Y., Gatti, D. L., Mitra, B., and Mathews, F. S. (2001) Structure of an active soluble mutant of the membrane-associated (*S*)-mandelate dehydrogenase. *Biochemistry 40*, 9870−9878.
(32) Ventura, M., Canchaya, C., Tauch, A., Chandra, G., Fitzgerald, G. F., Chater, K. F., and van Sinderen, D. (2007) Genomics of Actinobacteria: tracing the evolutionary history of an ancient phylum. *Microbiol. Mol. Biol. Rev. 71*, 495−548.
(33) Tartof, K. E., and Hobbs, C. A. (1987) Improved media for growing plasmid and cosmid clones. *Bethesda Res. Lab. Focus 9*, 2−12.
(34) Studier, F. W. (2005) Protein production by auto-induction in high-density shaking cultures. *Protein Expression Purif. 41*, 207−234.
(35) Lehoux, I. E., and Mitra, B. (1999) (*S*)-Mandelate dehydrogenase from *Pseudomonas putida*: mutations of the catalytic base histidine-274 and chemical rescue of activity. *Biochemistry 38*, 9948−9955.
(36) Tamura, Y., Ohkubo, A., Iwai, S., Wada, Y., Shinoda, T., Arai, K., Mineki, S., Iida, M., and Taguchi, H. (2002) Two forms of NAD-dependent D-mandelate dehydrogenase in *Enterococcus faecalis* IAM 10071. *Appl. Environ. Microbiol. 68*, 947−951.
(37) Dewanti, A. R., Xu, Y., and Mitra, B. (2004) Role of glycine 81 in (*S*)-mandelate dehydrogenase from *Pseudomonas putida* in substrate specificity and oxidase activity. *Biochemistry 43*, 10692−10700.
(38) Studier, F. W., and Moffatt, B. A. (1986) Use of bacteriophage T7 RNA polymerase to direct selective high-level expression of cloned genes. *J. Mol. Biol. 189*, 113−130.
(39) Sambrook, J. J., and Russell, D. D. W. (2001) *Molecular Cloning: A Laboratory Manual*, 3rd ed., p 2344, Cold Spring Harbor Laboratory Press, Cold Spring Harbor, NY.
(40) MacNeil, D. J., Occi, J. L., Gewain, K. M., MacNeil, T., Gibbons, P. H., Ruby, C. L., and Danis, S. J. (1992) Complex organization of *Streptomyces avermitifis* genes encoding the avermectin polyketide synthase. *Gene 115*, 119−125.
(41) Weaver, D., Karoonuthaisiri, N., Tsai, H., Huang, C., Ho, M., Gai, S., Patel, K. G., Huang, J., Cohen, S. N., Hopwood, D. A., Chen,

DOI: 10.1021/sb500368w
ACS Synth. Biol. 2015, 4, 796−807

C. W., and Kao, C. M. (2004) Genome plasticity in *Streptomyces*: identification of 1 Mb TIRs in the *S. coelicolor* A3 (2) chromosome. *Mol. Microbiol. 51*, 1535−1550.
(42) Gomez-Escribano, J. P., and Bibb, M. J. (2011) Engineering *Streptomyces coelicolor* for heterologous expression of secondary metabolite gene clusters. *Microb. Biotechnol. 4*, 207−215.
(43) Kieser, T., Bibb, M. J., Buttner, M. J., Chater, K. F., and Hopwood, D. A. (2000) *Practical Streptomyces Genetics*, p 613, The John Innes Foundation, Norwich, UK.
(44) Hong, H. J., Hutchings, M. I., Hill, L. M., and Buttner, M. J. (2005) The role of the novel Fem protein VanK in vancomycin resistance in *Streptomyces coelicolor*. *J. Biol. Chem. 280*, 13055−13061.
(45) Flett, F., Mersinias, V., and Smith, C. P. (1997) High efficiency intergeneric conjugal transfer of plasmid DNA from *Escherichia coli* to methyl DNA-restricting streptomycetes. *FEMS Microbiol. Lett. 155*, 223−229.
(46) Takano, E., Gramajo, H. C., Strauch, E., Andres, N., White, J., and Bibb, M. J. (1992) Transcriptional regulation of the *redD* transcriptional activator gene accounts for growth-phase-dependent production of the antibiotic undecylprodigiosin in *Streptomyces coelicolor* A3(2). *Mol. Microbiol. 6*, 2797−2804.
(47) Nakamura, L. K., Roberts, M. S., and Cohan, F. M. (1999) Relationship of *Bacillus subtilis* clades associated with strains 168 and W23: a proposal for *Bacillus subtilis* subsp. *subtilis spizizenii* subsp. *nov*. *Int. J. Syst. Bacteriol. 49*, 1211−1215.
(48) Berman, H. M., Westbrook, J., Feng, Z., Gilliland, G., Bhat, T. N., Weissig, H., Shindyalov, I. N., and Bourne, P. E. (2000) The Protein Data Bank. *Nucleic Acids Res. 28*, 235−242.
(49) Bairoch, A., and Apweiler, R. (1999) The SWISS-PROT protein sequence data bank and its supplement TrEMBL in 1999. *Nucleic Acids Res. 27*, 49−54.
(50) Kiziak, C., Conradt, D., Stolz, A., Mattes, R., and Klein, J. (2005) Nitrilase from *Pseudomonas fluorescens* EBC191: cloning and heterologous expression of the gene and biochemical characterization of the recombinant enzyme. *Microbiology 151*, 3639−3648.
(51) Edgar, R. C. (2004) MUSCLE: multiple sequence alignment with high accuracy and high throughput. *Nucleic Acids Res. 32*, 1792−1797.
(52) Saitou, N., and Nei, M. (1987) The neighbor-joining method: a new method for reconstructing phylogenetic trees. *Mol. Biol. Evol. 4*, 406−425.
(53) Felsenstein, J. (1985) Confidence limits on phylogenies: an approach using the bootstrap. *Evolution 39*, 783−791.
(54) Fernández-Martínez, L. T., Del Sol, R., Evans, M. C., Fielding, S., Herron, P. R., Chandra, G., and Dyson, P. J. (2011) A transposon insertion single-gene knockout library and new ordered cosmid library for the model organism *Streptomyces coelicolor* A3(2). *Antonie van Leeuwenhoek 99*, 515−522.
(55) Tedeschi, G., Pollegioni, L., and Negri, A. (2012) Assays of D-amino acid oxidases. *Methods Mol. Biol. 794*, 381−395.
(56) Thirlway, J., Lewis, R., Nunns, L., Al Nakeeb, M., Styles, M., Struck, A. W., Smith, C. P., and Micklefield, J. (2012) Introduction of a non-natural amino acid into a nonribosomal peptide antibiotic by modification of adenylation domain specificity. *Angew. Chem., Int. Ed. 51*, 7181−7184.

DOI: 10.1021/sb500368w
ACS Synth. Biol. 2015, 4, 796−807